



Decoupling filamentous phage uptake and energy of the TolQRA motor in *Escherichia coli* .

Poutoum Samire, Bastien Serrano, Denis Duché, Emeline Lemarie, Roland Llobes, Laetitia Houot

► To cite this version:

Poutoum Samire, Bastien Serrano, Denis Duché, Emeline Lemarie, Roland Llobes, et al.. Decoupling filamentous phage uptake and energy of the TolQRA motor in *Escherichia coli* .. Journal of Bacteriology, 2019, 10.1128/JB.00428-19 . hal-02336657

HAL Id: hal-02336657

<https://hal.science/hal-02336657>

Submitted on 6 Feb 2020

HAL is a multi-disciplinary open access archive for the deposit and dissemination of scientific research documents, whether they are published or not. The documents may come from teaching and research institutions in France or abroad, or from public or private research centers.

L'archive ouverte pluridisciplinaire **HAL**, est destinée au dépôt et à la diffusion de documents scientifiques de niveau recherche, publiés ou non, émanant des établissements d'enseignement et de recherche français ou étrangers, des laboratoires publics ou privés.

Decoupling filamentous phage uptake and energy of the TolQRA motor in *Escherichia coli*.

Poutoum SAMIRE*, Bastien SERRANO, Denis DUCHE, Emeline LEMARIE, Roland LLOUBES, Laetitia HOUOT[#]

Laboratoire d'Ingénierie des Systèmes Macromoléculaires, UMR7255, Institut de Microbiologie de la Méditerranée, Aix-Marseille Univ – CNRS, 31 Chemin Joseph Aiguier, CS 70071, 13402 Marseille Cedex 09, France.

Running title: Uptake of Fd phages by energy-deprived Tol system.

[#] Address correspondence to Dr. Laetitia Houot, lhouot@imm.cnrs.fr, tel: +33 (0)4 91 16 46 63, fax: +33 (0)4 91 71 21 24

*Present address: Biosciences and Biotechnologies Institute of Aix-Marseille (BIAM), Commissariat à l'Energie Atomique et aux Energies Alternatives (CEA), CNRS and Aix-Marseille University, UMR7265 EBM, CEA Cadarache, F-13108, Saint-Paul-lez-Durance, France

ABSTRACT

Filamentous phages are non-lytic viruses that specifically infect bacteria, establishing a persistent association with their host. The phage particle has no machinery for generating energy and parasitizes its host existing structures in order to cross the bacterial envelope and deliver its genetic material. The import of filamentous phages across the bacterial periplasmic space requires some of the components of a macro-complex of the envelope known as the Tol system. This complex uses the energy provided by the proton-motive force of the inner membrane to perform essential and highly energy-consuming functions of the cell, such as envelope integrity maintenance and cell division. It has been suggested that phages take advantage of pmf-driven conformational changes in the Tol system to transit across the periplasm. However, this hypothesis has not been formally tested. In order to decouple the role of the Tol system in cell physiology and during phage parasitism, we used mutations on conserved essential residues known for inactivating pmf-dependent functions of the Tol system. We identified impaired Tol complexes that remain fully efficient for filamentous phage uptake. We further demonstrate that the TolQ-TolR homologous motor, ExbB-ExbD, normally operating with the TonB protein, is able to promote phage infection along with full length TolA.

IMPORTANCE (120 mots)

Filamentous phages are widely distributed symbionts of gram-negative bacteria, some of them being linked to genome evolution and virulence of their host. However, the precise mechanism that permit their uptake across the cell envelope is poorly understood. The canonical phage model Fd requires the TolQRA protein complex in the host envelope, which is suspected to translocate proton across the inner membrane. In this study, we show that phage uptake proceeds in the presence of assembled but non-functional TolQRA complex. Moreover, our results unravel an alternative route for phage import that relies on the ExbB-ExbD proteins.

This work provides new insights into the fundamental mechanisms of phage infection, and might be generalized to other filamentous phages responsible for pathogen emergence.

KEYWORDS

bacteriophage, proton motive force, Tol-Pal system, Ton system, molecular motor.

INTRODUCTION

Living cells produce various sources of energy in order to sustain essential reactions and physiological functions. In Gram negative bacteria, the envelope is the location of heavy energetic processes. It is composed of two hydrophobic bilayers of lipids, the inner (IM) and outer-membrane (OM), imbedded with or associated to numerous proteins. The two membranes delimit the periplasmic space, an aqueous compartment containing a thin layer of peptidoglycan (PG), and devoid of adenosine triphosphate (ATP). The ionic gradients across the IM constitute the proton-motive force (pmf) and power a variety of dynamic processes that are essential for cell survival and multiplication, including ATP synthesis, flagellar rotation, energization of OM transporters and trafficking of molecules against a concentration gradient (1–3). The protein complexes that convert the electrochemical energy into mechanical movements are referred to as molecular motors and are thought to cycle like gears between energized and non-energized states. One of the best characterized pmf-energized motor is the MotA/MotB IM complex that powers the rotation of the bacterial flagellum (2).

Filamentous phages are obligate parasites of Gram-negative bacteria that deliver their genetic material from one susceptible bacterial cell to another in order to replicate. However, phages have no protein machinery for generating energy (4, 5). While more than 70 different filamentous phages have been reported in the literature, the understanding of the host infection

process is largely based on two types of viruses. Ff coliphages include fd, M13 and f1, and specifically infect *Escherichia coli* cells. They have served the development of extensive applications in genetic engineering and phage display technology (4, 5). CTX vibriophage carries the genes encoding the cholera toxin in its genome and converts *Vibrio cholerae* to a deadly pathogen upon infection (6). In both cases, the general mechanism of filamentous phage infection involves the phage minor coat protein pIII located at the tip of the particle and two sequential receptors of the host: a type-IV pilus, which is somehow dispensable but increases the phage infection efficiency, and the TolQRA proteins which are absolutely required for phage uptake (7–10). First, the phage specifically binds to the tip of the pilus protruding from the host cell surface (reception step) thanks to the central domain of pIII (pIII-N2) (11, 12). Pili are dynamic structures that normally undergo cycles of extension and retraction driven by ATPase activity at the cytoplasmic side of the IM (13). It is thought that coliphages like Fd and CTX vibriophage are brought close to the OM following pilus retraction of their target host (F-pilus and Toxin-coregulated pilus TCP, respectively) in a process that might not require ATP hydrolysis (14–16).

Once in the periplasmic space, filamentous phages require both TolA, TolQ and TolR for efficient infection (translocation step) (7, 8, 12, 17, 18). A direct interaction between TolA C-terminal domain (TolAIII) and the phage pIII-N-terminal domain (pIII-N1) has been documented (19–23), while the role of TolQ and TolR proteins remains unclear. TolA, TolQ and TolR proteins are part of the Tol-Pal system, a pmf-dependent molecular motor conserved in Gram-negative bacteria. It is involved in maintaining OM integrity, in OM lipid homeostasis and in the late stages of cell division (Fig. 1) (24–32). TolA is the central hub of the system. It is anchored to the IM thanks to a transmembrane (TM) domain and protrudes in the cell periplasmic space with a predicted long helical domain (TolAII) and a globular C-terminal domain (TolAIII). Besides TolA, the complex is composed of TolQ and TolR, which are

97 embedded in the IM thanks to three and one TM domains, respectively. TolQ and TolR both
98 interact with the TM domain of TolA, forming an IM subcomplex with a stoichiometry of four-
99 to-six TolQ, two TolR and one TolA (33–37). The OM associated subcomplex is composed of
100 the peptidoglycan associated lipoprotein (Pal) and the periplasmic protein TolB (38–40). TolQ
101 and TolR are thought to form an ion channel at the protein TM helix interfaces, which allows
102 the flow of protons from the periplasm to the cytoplasm (Fig. 1). As TolQ, TolR and TolA
103 interact in the IM, it is believed that the use of the pmf by the TolQ-TolR motor results in a
104 conversion of the electrochemical potential into mechanical movements that will eventually
105 trigger the stretch of TolAII across the periplasm and conformational changes in TolAIII. This
106 leads to the formation of a transient TolAIII-Pal complex that has been observed by co-
107 immunoprecipitation experiments *in vivo* (40). The system may alternate cycles of TolA–Pal
108 binding and release, coordinated with the pmf-induced mechanical movements occurring in the
109 IM subcomplex TolQ-TolR-TolA (41, 42). Deletion of one of the Tol proteins or dissipation of
110 the pmf with the protonophore CCCP (carbonyl cyanide m-chlorophenylhydrazone) abolishes
111 the link between the IM and OM Tol subcomplexes (40), resulting in pleiotropic *tol*⁻
112 phenotypes, such as high sensitivity to detergents and chaining morphology under low
113 osmolarity growth conditions (26).

114 The TolQR motor is evolutionary related to the pmf-dependent MotA-MotB motor generating
115 the rotation of the flagellum and the AglR-AglS-AglQ system energizing a gliding motility
116 machinery (36, 43). It also shares homologies with the ExbB-ExbD motor that energizes the
117 TonB protein and is responsible for the energy-dependent uptake of iron-charged siderophores
118 and vitamin B12 (Fig. 1A) (36, 44, 45). The Ton system has also recently been shown to be
119 involved in the secretion of a protease (46). Similarly to TolA being energized by the TolQR
120 motor, ExbBD transduces the energy derived from the pmf of the IM to generate conformational

changes into TonB, that are required for active transport through the TonB-dependent transporters (47, 48).

Tol and Ton systems are both parasitized by bacterial toxins called colicins. These small proteins, produced by and active against *Escherichia coli* strains, are classified as Group A and Group B. Group A colicins, such as ColA or ColE1, use a subset of the TolQRAB proteins, whereas group B colicins, such as ColB, use the ExbBD-TonB proteins to penetrate and kill their target bacteria. It is thought that some colicins depend on energy-induced conformational changes in the Tol or Ton system to perform translocation while other are still active in energy-deprived systems (26, 49, 50).

Filamentous phage translocation across the envelope has been suggested to require active pulling driven by pmf-induced conformation cycling of Tol system. Indeed, phage infection requires the host protein TolA, TolQ and TolR, which are part of a macrocomplex that uses the pmf for its normal functions. Moreover, cells exposure to the protonophore CCCP, able to dissipate the pmf, has been reported to strongly affect CTX phage transduction in *V. cholerae* (51). However, this chemical treatment is rather nonspecific as it acts at the whole-cell scale, and cannot differentiate between the energy requirement for pilus assembly and maintenance at the cell surface, pilus retraction and disassembly, and periplasmic transit of the phage particle.

In this study we aimed to investigate the requirements for phage translocation across the host periplasm using a genetic targeted approach. We and others have previously identified polar residues on specific faces of the TolQ and TolR TM helices (Fig. 1B) that are essential for pmf-dependent functions of the Tol system (36, 42, 52). These residues are conserved within the TolQ or TolR protein families but also in the homologous bacterial motors ExbB-ExbD, AlgR-AglS and MotA-MotB proteins. We specifically targeted residues in the TM helices of TolQ, TolR or TolA in order to affect the assembly of the TolQR-TolA IM complex, to abolish

pmf-dependent functions of the TolQR motor, or to impair energy transduction from TolQR to the phage receptor protein TolA. We also questioned if the ExbBD motor could be exchangeable with the TolQR motor for phage uptake.

RESULTS AND DISCUSSION

E. coli GM1 *tol* mutants display typical phenotypes

Filamentous phage uptake in *E. coli* requires the F-conjugative pilus at the surface of the bacterium as primary receptor (reception) and the TolQRA proteins in the envelope as secondary receptor (translocation). *tol* mutants have been reported to be unaffected for both the synthesis of F-pili, as well as the ability to undergo conjugation. Finally, the Leviviridae icosahedral phage f2, import of which is dependent on the F-pilus but independent of the Tol system, is still able to infect *E. coli* Tol-defective mutants (53). These features allow the study of filamentous phage translocation in the periplasm of wild-type and *tol* mutant strains independently of the initial F-pilus dependent reception step. We first generated various *E. coli* GM1 F-piliated strains lacking *tolA*, *tolQ-tolR* (referred later as $\Delta tolQR$ mutant) and *exbB-exbD* ($\Delta exbBD$ mutant) genes by P1 transduction and verified that they displayed typical phenotypes of *tol* and *exb* mutants. Compared to the GM1 wild-type strain, *tol* mutants showed an increased sensitivity to SDS (Fig. 2A), consistent with defects in the maintenance of OM integrity, and resistance to two Tol-dependent colicins: ColA (dependent on TolA, TolB, TolQ and TolR) and ColE1 (dependent on TolA and TolQ), (Fig. 2B). As expected, the quadruple mutant $\Delta tolQR\Delta exbBD$ was resistant to ColA and ColE1, as well as to the TonB-ExbBD dependent colicin ColB (Fig. 2B). The mutant phenotypes were rescued by ectopic expression from compatible vectors of the wild type copy of *tolA*, *tolQR* or *exbBD* genes, as indicated (Fig. 2 and supplemental data 1).

Phage infection occurs at low frequency in *E. coli tolQ* and *tolR* mutants, but not in *tolA* mutant.

Filamentous phages have been proposed to hijack TolA, TolQ and TolR proteins in order to transit across the periplasm of their target host and to position themselves for DNA ejection into the cytoplasm. So far, TolA is the only protein that has shown direct interaction with the phage in the periplasm (9). In *E. coli*, the deletion of *tolQ* or *tolR* was reported to totally abolish Ff phage infection, similarly to a *tolA* mutant (7, 8, 10, 53, 54). However in *V. cholerae*, *tolA* deletion results in a CTX phage resistant strain, while *tolQ* or *tolR* can still be infected at low frequency (17). These discrepancies might reflect differences in previous experimental setups used to conduct phage infection assays. In this study, we measured phage infection frequency in the different *E. coli* GM1 strain backgrounds using Fd-Tc coliphages carrying a tetracyclin resistant marker. In order to increase the sensitivity of our assay, we used a high multiplicity of infection with the aim to saturate the phage entrance pathway in the host cell (infection frequency $>10^{-1}$ for the wild type strain, Fig. 3). With this experimental setup, we observed that the GM1 $\Delta tolA$ mutant was fully resistant to phage infection (infection frequency below the detection threshold of 1.10^{-6}), while a $\Delta tolQR$ mutant remained susceptible to the Fd-Tc phage, albeit a 5 log decrease in infection efficiency compared to the wild-type strain (Fig. 3A). As a control, we verified the abundance of TolA in a $\Delta tolQR$ mutant compared to the WT strain (Supplemental data 2). The *tolQR* deletion resulted in a slight decrease in the total amount of TolA in all the tested strain, even when fully complemented with the pTolQR plasmid for the tested phenotypes (Fig. 2). This suggests that the decrease in phage susceptibility in $\Delta tolQR$ mutant was not the result of the decrease in the abundance of its receptor TolA. We concluded that the Fd phage strictly requires the host receptor TolA, while TolQ and TolR are important but not essential for efficient infection.

The ExbBD motor can partially replace the TolQR motor for phage uptake but not for maintaining OM integrity.

Because a low level of infection is still observed in a $\Delta tolQR$ mutant (Fig. 3A), we hypothesized that the phage receptor TolA might be functioning with another IM related system in absence of the TolQ-TolR complex. ExbB-ExbD and TolQ-TolR motors share structural and functional homologies and have been reported to perform crosstalk. Indeed, the TolQR complex can partially replace the ExbBD motor to energize TonB and to couple the energy of the pmf with OM transport cycle of vitamin B12 (55) and with Ton-dependent colicin uptake. However, the reciprocal complementation of a TolQR mutant by the endogenous ExbBD motor do not support Tol-dependent OM integrity (for review, see (26) and Fig. 2B). In the case of a crosstalk between the two systems for Fd phage uptake, we would expect to totally abolish phage infection in a quadruple mutant deleted of *tolQ*, *tolR*, *exbB* and *exbD*. Indeed, the $\Delta tolQR$ -*exbBD* mutant was fully resistant to phage infection, as shown in Fig. 3B. Moreover, we observed that overexpressing the ExbB-ExbD encoding genes from a plasmid in a $\Delta tolQR$ -*exbBD* mutant background promoted phage uptake to the wild-type level (Fig. 3B), as well as Colicin E1 killing (Fig. 2B). As ColE1 import relies on TolA and TolQ but not TolR, and consequently is thought to be energy independent, this data also suggests that ExbB can partially replace TolQ in the ColE1 translocation pathway. Of note, ExbB-ExbD protein did not cross-complement the mutant strain for ColicinA uptake, which is consistent with a previous study reporting that ColA translocation in the host requires a direct interaction with TolR (56). On the contrary, cells producing TolA with the ExbBD complex were sensitive to SDS, suggesting that pmf-dependent OM integrity is still impaired in this background (Fig. 2A). Taken together, these phenotypes suggest that in the absence of TolQR, the phage uses the

ExbBD complex along with TolA as an alternative route to perform its translocation in the host envelope, in a process that is not coupled to normal functioning of the Tol system.

The phage receptor domain TolAIII is strictly required but not sufficient for phage uptake.

We then questioned if the isolated phage receptor domain TolAIII, and the TolQR complex would be sufficient for processing the uptake of the phage particle across the periplasmic space. Indeed, TolAIII is sufficient for binding Fd phage protein pIII-N1 *in vitro* (19, 23) and in a bacterial 2-hybrid assay (21). It was also shown that overexpressing the isolated TolAIII domain in the host periplasm disturbs the normal functioning of the Tol system, and decreases cell susceptibility to phage infection, possibly by sequestering the phage in the periplasm and preventing the infection to proceed to the next step (7). Using a similar approach in Fig. 4, we expressed the isolated TolAIII domain in the WT and in the $\Delta tolA$ cell periplasm using a pIN-III-ompA2 vector carrying a fusion between the sec-dependent *ompA* signal sequence and the *tolAIII* sequence (57). As a control, we used the pIN-pIII^{ΔYGT} vector that has been previously reported to produce an inactive pIII variant, unable to bind TolA in the periplasm (58). We first verified that periplasmic production of TolAIII in the WT strain impaired the ability of the cell to resist to SDS (Fig. 4A), and decreased the frequency of infection by Fd-Tc (Fig. 4B), while periplasmic production of the control pIII^{ΔYGT} had no effect. Then, we used the pIN-TolAIII vector to produce TolAIII in the periplasm of GM1 $\Delta tolA$ cells and measured the frequency of Fd phage infection in this background. The TolAIII domain did not allow phage uptake despite the presence of the endogenous TolQR motor, and contrary to the full-length TolA protein. We concluded that TolAIII deprived of its TM domain TolAI and periplasmic helical stretch TolAII is not sufficient for infection. This suggests that TolAI and/or TolAII also participate in the uptake process. Consistent with this hypothesis, an interaction assay conducted on isolated

domains by SPR analysis reported that TolAII binds the phage pIII-N2 domain with an apparent affinity of 1.3 to 2.4 μ M (59). However, the significance of this interaction is unclear, as deletion of the full helical domain TolAII reduced the efficiency of infection by a 5.5 factor, but do not abolish it (7). It has been shown that TolAIII exists as different conformations depending on the interaction of TolAI with the TolQR complex in the IM and the energetic-status of the cell (36, 40, 52). Thus, TolAII might serve as a dynamic spring, transducing mechanical movements from its IM anchor TolAI that will eventually facilitate TolAIII positioning in the periplasm for efficient phage translocation.

Phage uptake requires interaction between TolA TM domain and TolQR.

We then questioned if TolA needed to be in interaction with TolQ and TolR in the IM to promote phage uptake. It has been previously reported that the TolQR complex assembles with TolA thanks to a conserved SHLS motif in the TolAI domain (52, 60, 61). Mutations of Ser18 or His22 residues in the TolA SHLS motif strongly impairs the interaction of TolA with the TolQ-TolR motor, as seen in an *in vivo* cross-linking experiment ((60) and supplemental data 3) and prevent energy-dependent conformational changes of TolA and interaction with Pal in the OM (52). We first constructed plasmids producing TolA carrying a S18W or a H22W mutation, and tested the ability of these variants to complement a $\Delta tolA$ mutant phenotype. The cells producing either TolA_{S18W} or TolA_{H22W} variants showed sensitivity to SDS, similarly to the $\Delta tolA$ mutant carrying a control plasmid (Fig. 5A), demonstrating that the mutations impair the ability of TolQ, TolR and TolA to form an assembled and functional IM complex. However, the TolA_{S18W} and TolA_{H22W} proteins were able to support colicin E1 entry (Fig. 5B), which is known to depend only on the presence of TolA and TolQ, independently of the energy-state of the Tol motor. Finally, the strains expressing the TolA_{S18W} or TolA_{H22W} proteins were more sensitive to TonB-dependent colicin B than the strain expressing wild-type TolA. This data is

consistent with the observation that mutations in TolA TM domain impair interaction with the TolQR motor (supplemental data 3), which may then become available to cross-complement the absence of ExbBD and to energize TonB, allowing ColB entry. Together, these data show that, contrary to the wild-type TolA, TolA_{S18W} and TolA_{H22W} variants are not properly assembled with the TolQR complex. Finally, we measured the frequency of phage infection in the GM1 cells expressing TolQR along with TolA_{S18W} or TolA_{H22W} proteins and found that they were less susceptible to phage infection (about 3 log decrease) compared to the cells expressing wild type TolA (Fig. 5C). This suggests that optimum phage uptake requires interaction of TolA with the TolQR complex in the IM. However, vanishing interactions between the TolA mutants and TolQR might be sufficient for low-frequency phage transduction, because uptake of a single phage results in the acquisition of the Tet-resistance cassette by the host. These phenotypes are reminiscent to those obtained when the endogenous ExbBD complex partially cross complement the absence of TolQR for TolA-dependent functions (Fig. 2 and Fig. 3).

Phage uptake proceeds in the presence of assembled but non-functional IM TolQRA complex.

We decided to further investigate whether Fd phages require that the Tol system is under a pmf-energized operating state to transit across the cell envelope, similarly to what has been described for Group B colicins that parasitize the homologous TonB-ExbBD system (49). It is thought that energization of the Tol-Pal system relies on an ion channel that forms at the TM interface between TolR and TolQ. The conversion of the electrochemical energy into mechanical movements in the Tol system involves the TolR_{D23}, TolQ_{T145}, and TolQ_{T178} polar residues, located in TolR TM, in TolQ TM2 and in TolQ TM3 segments, respectively (41, 42) (Fig. 1B). *Mutation of TolR D23 residue.* The Asp23 in TolR has been proposed to be the key ionizable residue of the channel, and is also present and essential to the function of the homologous ExbD

(Asp25), AglQ (Asp28), AglS (Asp41) and MotB (Asp32) proteins (2, 43). In cells producing a TolR_{D23C} variant, the IM TolA-TolQ-TolR_{D23C} complex is assembled (41) (supplemental data 3) but totally defective for both energy dependent and energy independent functions. Indeed, the TolQ-TolR_{D23C} motor is unable to promote the interaction between TolA and Pal anchored in the OM, resulting in *tol*⁻ phenotypes (41, 42, 62). In our experiments, rescue of the $\Delta tolQR$ $\Delta tolA\Delta exbBD$ mutant was not observed with ectopic expression of the *tolR_{D23C}* variant along with WT copies of TolA and TolQ (Fig. 5), despite correct expression of the proteins (supplemental data 1 and supplemental data 3). We verified that this result was not caused by a pmf defect at the whole cell level, as inactivating both the TolQRA and the ExbBD systems does not significantly disturb the membrane potential compared to the WT cells (supplemental figure 4).

Finally, we found that filamentous phages were unable to penetrate the cells producing the TolQ-TolR_{D23C}-TolA complex. We hypothesize that in this energy-less state of the motor, TolA conformation prevents its binding to the phage, or alternatively, that the phage is stuck in the periplasm and cannot progress in the translocation pathway.

Mutation of TolQ threonine 145 and 178 residues. Finally, we took advantage of mutants TolQ_{T145A}, and TolQ_{T178A} that have been reported to present discriminative phenotypes (62). In these backgrounds, the state of the motor differs from the TolQ-TolR_{D23C}-TolA, as the system is defective (TolA does not bind to Pal *in vivo*) but can still support pmf-independent processes like colicin uptake (62). As expected, the cells expressing either the TolQ_{T145A} or TolQ_{T178A} variants were sensitive to SDS but were still able to be killed by ColA and ColE1 (Fig. 5A and B). It is interesting to note that, contrary to wild-type TolQ, these two mutants are unable to perform crosstalk for ColB uptake (Fig. 5B), which requires a pmf-energized state of TonB, consistently with the hypothesis that the motors composed of TolR and TolQ_{T145A} or TolQ_{T178A} variants are unable to transduce energy to a partner. Finally, we observed that filamentous

phages were able to infect cells expressing the TolQ_{T145A} or TolQ_{T178A} variants at a frequency similar to the WT strain. We concluded that Fd phage translocation in the host periplasm not dependent on a functional TolQRA system. Thus, our data challenge the model that filamentous phages use the energy-dependent pulling-action and cycling of TolA to cross the periplasm and reach the IM.

The data presented here have to be interpreted in the context of normal functioning of the Tol-Pal system for OM maintenance and during cell division. Indeed, it has been speculated that TolA cycles between different conformations, depending on its energized or non-energized states regulated by the TolQR motor, similarly to TonB energized by the ExbBD motor (65). In the current working model, energy-loaded TolA interacts with the OM lipoprotein Pal, bridging the IM and the OM layers. During cell division, conformational changes in the Tol system provides the energy needed for the OM to be pulled towards the pinch point (29, 32). The mechanisms allowing progression of OM invagination remain to be fully elucidated, but might require cycles of TolA–Pal interaction and release. Taken together, our data on TolR_{D23}, TolQ_{T145} and TolQ_{T178} highlight the existence of distinct non-functional states of the TolQRA complex that might reflect sequential steps in motor cycling, coordinated with the ion conduction pathway inside the complex. It also suggests that phage import requires assembly and initial activation state of the TolQRA complex, that cannot be reached when TolR Asp23 residue is mutated. At this point, it is unclear if this initial activation step of the TolQRA complex is dependent on proton progression in the motor channel or not. Previous data on *V. cholerae* showed that dissipation of the pmf by the protonophore CCCP abolishes CTX phage infection (51). It is possible that CCCP treatment results in a non-functional TolQR complex that blocks TolA in a conformation that is not able to support phage translocation in the periplasm. This frozen state might be similar to the one obtained when TolA interacts with the TolR_{D23C} variant protein (Fig. 5). An alternative explanation could be that CCCP treatment

impacts other mechanisms, upstream or downstream the Tol-reception step. Indeed, both pmf and ATP depletion can be observed following CCCP treatment (64). Moreover, exposure to CCCP has been reported to decrease the total number of F-pili extruding from the cell surface (65), and eclipse of the F-pili is an ATP-requiring process, that could be impacted by a general decrease of the pmf. Finally, opening of the phage head particle at the OM and final DNA injection in the cytoplasm might require the presence of a pmf across the cytoplasmic membrane of the host cell, as reported for T4 phage (66). While pmf does not seem to power phage translocation, this energy could serve other steps of the process, such as pilus retraction or opening of the phage particle head in the IM. Alternatively, the data might reflect the high energy requirement for cell OM integrity maintenance, that cannot be reached when TolA operates with the TolQ_{T145A} or TolQ_{T178A} variants, or with the homologous ExbBD motor. In this case, the defective Tol IM complexes could either operate with a very slow cycling or poor torque. Measuring the effect of TolQ or TolR point mutations on channel conductance would help the understanding of the different stages in the Tol motor cycling, but requires reconstitution of the system *in vitro* (for example in planar lipid bilayers). While this approach has been set up for the homologous motor ExbB-ExbD (44, 67), it has not been set up for the TolQ-TolR system so far.

In conclusion, our data demonstrate that filamentous Fd phage transit in the periplasm requires the presence of an assembled TolQ-TolR-TolA complex anchored to the IM. The system need to reach a first activation state (depending on TolR Asp23 residue), but does not require to be functional to promote phage uptake (as attested by TolQ T145 and T178 variants). We also show that the homologous ExbBD complex can support phage uptake along with TolA in the absence of the TolQR complex. Although a detailed mechanical analysis of the Tol proteins is beyond the scope of this study, it would be of great interest to understand the structural and dynamic basis for the coordination between the phage particle and the Tol

components during cell cycle. As some the filamentous phages are linked to the pathogenicity potential of their host, deciphering the energy requirements for these potentially important bacterial parasites might lead to novel intervention strategies.

Materials and Methods

Bacterial strains and growth conditions— Bacterial strains and plasmids used in this study are listed in Supplemental Table S1. Bacteria were cultivated in Luria-Bertani broth (LB) at 37°C. When indicated, antibiotics were added to the medium at the following concentrations: streptomycin (100 µg/ml), ampicillin (50 or 100 µg/ml), kanamycin (50 µg/ml), tetracyclin (15 µg/ml). For *E. coli* GM1 deletion strains, the recombinant genes were transferred from W3110 strain (32) to the desired strain background by P1 transduction (68).

Plasmid construction. Polymerase Chain Reactions (PCR) were performed using Q5 High Fidelity DNA polymerase (NewEngland Biolabs). Primer sets required to generate genetic constructs were synthesized by Sigma Aldrich. Enzymes (NewEngland Biolabs) were used according to the manufacturer's instructions. Plasmids were constructed using standard cloning techniques, as previously described (21, 41). Mutations on pBAD-*tolQR* and pOK*tolA* plasmids were performed by Quick-change site-directed mutagenesis using complementary pairs of oligonucleotides (listed in Table S2) and Pfu Turbo polymerase. All constructs were confirmed by DNA sequencing (Eurofins, MWG).

SDS-PAGE and Immunoblotting— Protein samples resuspended in 2x loading buffer (Tris-HCl 100 mM pH=6.8, SDS 2%, glycérol 10%, bromophenol blue 0.01 %, 5% 2-βmercaptoéthanol) were subjected to sodium dodecyl sulphate (SDS)-polyacrylamide gel electrophoresis (PAGE). For detection by immunostaining, proteins were transferred onto nitrocellulose membranes, and

immunoblots were probed with primary antibodies, and goat secondary antibodies coupled to alkaline phosphatase, and developed in alkaline buffer in presence of 5-bromo-4-chloro-3-indolylphosphate (BCIP) and nitroblue tetrazolium (NBT). The anti-TolAIII and anti-TolR polyclonal antibodies are from our laboratory collection while the anti-HA monoclonal antibody (Invitrogen), and alkaline phosphatase-conjugated goat anti-rabbit and anti-mouse antibodies (Millipore) have been purchased as indicated.

Phenotypic analysis—

Sensitivity test to SDS. Cells harboring the empty plasmid as a control, or the plasmid encoding the constructs of interest were grown in LB medium until stationary phase, then back diluted 100x in LB supplemented with L-arabinose 0.02% or IPTG 100 μ M if necessary. After 1hr incubation at 37°C, cultures were adjusted to OD_{600nm}=0.2 in LB supplemented or not with SDS 0.2%, and transferred to a 96 wells plate (final volume of 300 μ L) and static grown for 5 hrs at 37°C. The OD_{600nm} was measured using a TECAN. The percentage of surviving cells was estimated from the turbidity ratio of the SDS-treated cells and the control samples. Experiments were performed in triplicates.

Colicin susceptibility. Colicin activities were observed by the presence of clear halos on a lawn of the strain to be tested, as described previously (56). Briefly, over-night cultures of the strains were spread on LB agar petri dishes supplemented with antibiotics and plasmid expression was induced as specified, using L-arabinose (0.02%) and IPTG (100 μ M). After drying, 1 μ L of serial dilutions (10 fold) of colicins was spotted on the bacterial lawn. Plates were incubated at 37°C for 16 hrs. The data are reported as the maximal dilution of the colicin stock sufficient for inhibiting cell growth. Experiments were conducted in duplicates.

Fd-Tc phage preparation and titration

A 5 mL preculture of GM1 strain was grown at 37°C. At $OD_{600nm} = 0.5$ to 0.6, it was inoculated with a colony of *E. coli* JM101 Fd-Tet (ATCC37000) and incubated for 2 hours at 37°C. The preculture was then used to inoculated a 500 ml culture of LB and incubated for 1 hour at 37°C with shaking. At this point, tetracyclin (15 µg/ ml) was added to select infected cells only. After overnight incubation at 30°C with shaking, the culture was centrifuged at 10,800 g for 15 min at 4 °C. The supernatant containing the phages was precipitated with 1/4V of a PEG/NaCl solution (20% Polyethylene glycol 8000; 2.5 M NaCl) for 2 hours on ice, and phages were collected by centrifugation at 10,800g for 30 min at 4°C. The pellet was resuspended in 8 ml PBS, and a second round of precipitation with 1/4V PEG/NaCl solution was performed 20 min on ice. The phage solution was centrifuged at 3,300 g for 30 min and the pellet was resuspended in 5 mL PBS. Remaining bacterial debris were removed by centrifuge at 11,600 g for 10 min and 0.2 µM seringe-filtration. Phage preparations were checked for sterility by plating on LB plate.

Titration of the phage suspension was performed as followed: the phage suspension was serial diluted in sterile PBS (10 fold). 10 µl of each phage dilution was incubated with 200 µl of GM1 receptor cells grown at $OD_{600nm} = 0.5$ to 0.6. After 30 min of incubation at room temperature without shaking, the cells were vortexed for 5s, and 5 µl were drops on a LB plate supplemented with Tc 15 ng/µl. After overnight incubation at 37°C, CFU were counted in the highest dilution test, leading to titer determination of 10^{13} to 10^{16} phages/ml.

Susceptibility to Fd-Tc phage infection assays.

Strains of interest were cultivated to reach $OD_{600nm} = 0.7$ to 0.8 and normalized to the same initial OD_{600nm} . 10 µl of phage suspension was added to 200 µL cells (multiplicity of infection of 10,000 phages per bacteria). Infection assay were performed in triplicate in 96-well plates, during 30 min of incubation at room temperature without shaking. The cells were vigorously

homogenized by pipetting, and immediately serial diluted 10 fold in sterile PBS. 5 µl were drops on a LB plate (total recipient CFU) or LB agar supplemented with Tc (15 ng/µl) (phage infected CFU). After overnight incubation at 37°C, isolated CFU were counted in the appropriate dilution test. The frequency of infection was determined by dividing the number of infected cells by the number of total recipient cells. Experiments were conducted in triplicates.

Acknowledgements— *We thank A. Brun, I. Bringer, M. Ba and O. Uderso for technical assistance, members of the LISM for helpful advices on the project, B. Ize for careful reading of the manuscript and Marc Hassein for encouragements. The pOKA plasmid was generously provided by Dr. A. Barnéoud-Arnoulet. Work in the laboratory is supported by the Centre National de la Recherche Scientifique (CNRS), the Aix-Marseille Univ. and by Agence Nationale de la Recherche (MEMOX, ANR-I8-CE11).*

Conflict of interest—The authors declare that they have no conflicts of interest with the contents of this article.

Bibliography

1. Noinaj N, Guillier M, Barnard TJ, Buchanan SK. 2010. TonB-dependent transporters: regulation, structure, and function. *Annu Rev Microbiol* 64:43–60.
2. Morimoto YV, Minamino T. 2014. Structure and function of the bi-directional bacterial flagellar motor. *Biomolecules* 4:217–234.
3. Guo H, Rubinstein JL. 2018. Cryo-EM of ATP synthases. *Curr Opin Struct Biol* 52:71–79.
4. Rakonjac J, Bennett NJ, Spagnuolo J, Gagic D, Russel M. 2011. Filamentous

470 bacteriophage: biology, phage display and nanotechnology applications. *Curr Issues Mol Biol*
471 13:51.

472 5. Loh B, Kuhn A, Leptihn S. 2018. The fascinating biology behind phage display:
473 filamentous phage assembly. *Mol Microbiol* 111:1132-1138.

474 6. Waldor MK, Mekalanos JJ. 1996. Lysogenic conversion by a filamentous phage
475 encoding cholera toxin. *Science* 272:1910–1914.

476 7. Click EM, Webster RE. 1997. Filamentous phage infection: required interactions with
477 the TolA protein. *J Bacteriol* 179:6464–6471.

478 8. Click EM, Webster RE. 1998. The TolQRA proteins are required for membrane
479 insertion of the major capsid protein of the filamentous phage f1 during infection. *J Bacteriol*
480 180:1723–1728.

481 9. Riechmann L, Holliger P. 1997. The C-terminal domain of TolA is the coreceptor for
482 filamentous phage infection of *E. coli*. *Cell* 90:351–360.

483 10. Russel M, Whirlow H, Sun TP, Webster RE. 1988. Low-frequency infection of F-
484 bacteria by transducing particles of filamentous bacteriophages. *J Bacteriol* 170:5312–5316.

485 11. Deng L-W, Perham RN. 2002. Delineating the Site of Interaction on the pIII Protein of
486 Filamentous Bacteriophage fd with the F-pilus of *Escherichia coli*. *J Mol Biol* 319:603–614.

487 12. Heilpern AJ, Waldor MK. 2003. pIIICTX, a predicted CTX minor coat protein, can
488 expand the host range of coliphage fd to include *Vibrio cholerae*. *J Bacteriol* 185:1037–1044.

489 13. McCallum M, Tammam S, Khan A, Burrows LL, Howell PL. 2017. The molecular
490 mechanism of the type IVa pilus motors. *Nat Commun* 8:15091.

491 14. Jacobson A. 1972. Role of F pili in the penetration of bacteriophage f1. *J Virol*
492 10:835–843.

493 15. Clarke M, Maddera L, Harris RL, Silverman PM. 2008. F-pili dynamics by live-cell
494 imaging. *Proc Natl Acad Sci USA* 105:17978–17981.

495 16. Ng D, Harn T, Altindal T, Kolappan S, Marles JM, Lala R, Spielman I, Gao Y, Hauke
496 CA, Kovacikova G, others. 2016. The *Vibrio cholerae* Minor Pilin TcpB Initiates Assembly
497 and Retraction of the Toxin-Coregulated Pilus. PLoS pathogens 12:e1006109.

498 17. Heilpern AJ, Waldor MK. 2000. CTX ϕ infection of *Vibrio cholerae* requires the
499 tolQRA gene products. J Bacteriol 182:1739–1747.

500 18. Sun TP, Webster RE. 1987. Nucleotide sequence of a gene cluster involved in entry of
501 E colicins and single-stranded DNA of infecting filamentous bacteriophages into *Escherichia*
502 *coli*. J Bacteriol 169:2667–2674.

503 19. Deprez C, Lloubès R, Gavioli M, Marion D, Guerlesquin F, Blanchard L. 2005.
504 Solution structure of the *E.coli* TolA C-terminal domain reveals conformational changes upon
505 binding to the phage g3p N-terminal domain. J Mol Biol 346:1047–1057.

506 20. Ford CG, Kolappan S, Phan HTH, Waldor MK, Winther-Larsen HC, Craig L. 2012.
507 Crystal structures of a CTX pIII domain unbound and in complex with a *Vibrio cholerae*
508 TolA domain reveal novel interaction interfaces. J Biol Chem 287:36258–36272.

509 21. Houot L, Navarro R, Nouailler M, Duché D, Guerlesquin F, Lloubes R. 2017.
510 Electrostatic interactions between the CTX phage minor coat protein and the bacterial host
511 receptor TolA drive the pathogenic conversion of *Vibrio cholerae*. J Biol Chem 292:13584–
512 13598.

513 22. Hecht O, Ridley H, Lakey JH, Moore GR. 2009. A common interaction for the entry
514 of colicin N and filamentous phage into *Escherichia coli*. J Mol Biol 388:880–893.

515 23. Lubkowski J, Hennecke F, Plückthun A, Wlodawer A. 1999. Filamentous phage
516 infection: crystal structure of g3p in complex with its coreceptor, the C-terminal domain of
517 TolA. Structure 7:711–722.

518 24. Yeh Y-C, Comolli LR, Downing KH, Shapiro L, McAdams HH. 2010. The
519 Caulobacter Tol-Pal complex is essential for outer membrane integrity and the positioning of

520 a polar localization factor. J Bacteriol 192:4847–4858.

521 25. Duché D, Houot L. 2019. Similarities and Differences between Colicin and
522 Filamentous Phage Uptake by Bacterial Cells. EcoSal Plus. doi: 10.1128/ecosalplus.

523 26. Lloubès R, Cascales E, Walburger A, Bouveret E, Lazdunski C, Bernadac A, Journet
524 L. 2001. The Tol-Pal proteins of the *Escherichia coli* cell envelope: an energized system
525 required for outer membrane integrity? Res Microbiol 152:523–529.

526 27. Bernadac A, Gavioli M, Lazzaroni JC, Raina S, Lloubès R. 1998. *Escherichia coli* tol-
527 pal mutants form outer membrane vesicles. J Bacteriol 180:4872–4878.

528 28. Meury J, Devilliers G. 1999. Impairment of cell division in tolA mutants of
529 *Escherichia coli* at low and high medium osmolarities. Biol Cell 91:67–75.

530 29. Gerding MA, Ogata Y, Pecora ND, Niki H, de Boer PAJ. 2007. The *trans* -envelope
531 Tol-Pal complex is part of the cell division machinery and required for proper outer-
532 membrane invagination during cell constriction in *E. coli*. Mol Microbiol 63:1008–1025.

533 30. Gray AN, Egan AJ, Van't Veer IL, Verheul J, Colavin A, Koumoutsis A, Biboy J,
534 Altelaar AM, Damen MJ, Huang KC, others. 2015. Coordination of peptidoglycan synthesis
535 and outer membrane constriction during *Escherichia coli* cell division. Elife 4:e07118.

536 31. Shrivastava R, Jiang X, Chng S-S. 2017. Outer membrane lipid homeostasis via
537 retrograde phospholipid transport in *Escherichia coli*. Mol Microbiol 106:395–408.

538 32. Petiti M, Serrano B, Faure L, Lloubes R, Mignot T, Duché D. 2019. Tol energy-driven
539 localization of Pal and anchoring to the peptidoglycan promote outer-membrane constriction.
540 J Mol Biol 431:3275-3288.

541 33. Derouiche R, Bénédicti H, Lazzaroni JC, Lazdunski C, Lloubès R. 1995. Protein
542 complex within *Escherichia coli* inner membrane. TolA N-terminal domain interacts with
543 TolQ and TolR proteins. J Biol Chem 270:11078–11084.

544 34. Journet L, Rigal A, Lazdunski C, Bénédicti H. 1999. Role of TolR N-terminal, central,

545 and C-terminal domains in dimerization and interaction with TolA and tolQ. J Bacteriol
546 181:4476–4484.

547 35. Lazzaroni JC, Vianney A, Popot JL, Bénédicti H, Samatey F, Lazdunski C, Portalier
548 R, Géli V. 1995. Transmembrane alpha-helix interactions are required for the functional
549 assembly of the *Escherichia coli* Tol complex. J Mol Biol 246:1–7.

550 36. Cascales E, Lloubes R, Sturgis JN. 2001. The TolQ–TolR proteins energize TolA and
551 share homologies with the flagellar motor proteins MotA–MotB. Mol Microbiol 42:795–807.

552 37. Vianney A, Lewin TM, Beyer WF, Lazzaroni JC, Portalier R, Webster RE. 1994.
553 Membrane topology and mutational analysis of the TolQ protein of *Escherichia coli* required
554 for the uptake of macromolecules and cell envelope integrity. J Bacteriol 176:822–829.

555 38. Clavel T, Germon P, Vianney A, Portalier R, Lazzaroni JC. 1998. TolB protein of
556 *Escherichia coli* K-12 interacts with the outer membrane peptidoglycan-associated proteins
557 Pal, Lpp and OmpA. Mol Microbiol 29:359–367.

558 39. Walburger A, Lazdunski C, Corda Y. 2002. The Tol/Pal system function requires an
559 interaction between the C-terminal domain of TolA and the N-terminal domain of TolB. Mol
560 Microbiol 44:695–708.

561 40. Cascales E, Gavioli M, Sturgis JN, Lloubès R. 2000. Proton motive force drives the
562 interaction of the inner membrane TolA and outer membrane pal proteins in *Escherichia coli*.
563 Mol Microbiol 38:904–915.

564 41. Zhang XY-Z, Goemaere EL, Thomé R, Gavioli M, Cascales E, Lloubès R. 2009.
565 Mapping the interactions between *Escherichia coli* Tol subunits: ROTATION OF THE TolR
566 TRANSMEMBRANE HELIX. J Biol Chem 284:4275–4282.

567 42. Goemaere EL, Devert A, Lloubes R, Cascales E. 2007. Movements of the TolR C-
568 terminal Domain Depend on TolQR Ionizable Key Residues and Regulate Activity of the Tol
569 Complex. J Biol Chem 282:17749–17757.

570 43. Agrebi R, Wartel M, Brochier-Armanet C, Mignot T. 2015. An evolutionary link
571 between capsular biogenesis and surface motility in bacteria. *Nat Rev Microbiol* 13:318–326.

572 44. Celia H, Noinaj N, Zakharov SD, Bordignon E, Botos I, Santamaria M, Barnard TJ,
573 Cramer WA, Lloubes R, Buchanan SK. 2016. Structural insight into the role of the Ton
574 complex in energy transduction. *Nature* 538:60–65.

575 45. Braun V, Herrmann C. 1993. Evolutionary relationship of uptake systems for
576 biopolymers in *Escherichia coli*: cross-complementation between the TonB-ExbB-ExbD and
577 the TolA-TolQ-TolR proteins. *Mol Microbiol* 8:261–268.

578 46. Gómez-Santos N, Glatter T, Koebnik R, Świątek-Połatyńska MA, Søgaard-Andersen
579 L. 2019. A TonB-dependent transporter is required for secretion of protease PopC across the
580 bacterial outer membrane. *Nat Commun* 10:1360.

581 47. Ollis AA, Postle K. 2012. ExbD mutants define initial stages in TonB energization. *J*
582 *Mol Biol* 415:237–247.

583 48. Ollis AA, Kumar A, Postle K. 2012. The ExbD periplasmic domain contains distinct
584 functional regions for two stages in TonB energization. *J Bacteriol* 194:3069–3077.

585 49. Cascales E, Buchanan SK, Duche D, Kleanthous C, Lloubes R, Postle K, Riley M,
586 Slatin S, Cavard D. 2007. Colicin Biology. *Microbiol Mol Biol Rev* 71:158–229.

587 50. Vankemmelbeke M, Zhang Y, Moore GR, Kleanthous C, Penfold CN, James R. 2009.
588 Energy-dependent immunity protein release during tol-dependent nuclease colicin
589 translocation. *J Biol Chem* 284:18932–18941.

590 51. Häse CC. 2003. Ion motive force dependence of protease secretion and phage
591 transduction in *Vibrio cholerae* and *Pseudomonas aeruginosa*. *FEMS Microbiol Lett* 227:65–
592 71.

593 52. Germon P, Ray MC, Vianney A, Lazzaroni JC. 2001. Energy-dependent
594 conformational change in the TolA protein of *Escherichia coli* involves its N-terminal

595 domain, TolQ, and TolR. J Bacteriol 183:4110–4114.

596 53. Sun TP, Webster RE. 1986. *fii*, a bacterial locus required for filamentous phage
597 infection and its relation to colicin-tolerant *tolA* and *tolB*. J Bacteriol 165:107–115.

598 54. Bradley DE, Whelan J. 1989. *Escherichia coli* *tolQ* mutants are resistant to
599 filamentous bacteriophages that adsorb to the tips, not the shafts, of conjugative pili. J Gen
600 Microbiol 135:1857–1863.

601 55. Bradbeer C. 1993. The proton motive force drives the outer membrane transport of
602 cobalamin in *Escherichia coli*. J Bacteriol 175:3146–3150.

603 56. Journet L, Bouveret E, Rigal A, Lloubes R, Lazdunski C, Bénédicti H. 2001. Import of
604 colicins across the outer membrane of *Escherichia coli* involves multiple protein interactions
605 in the periplasm. Mol Microbiol 42:331–344.

606 57. Bouveret E, Journet L, Walburger A, Cascales E, Bénédicti H, Lloubès R. 2002.
607 Analysis of the *Escherichia coli* Tol-Pal and TonB systems by periplasmic production of Tol,
608 TonB, colicin, or phage capsid soluble domains. Biochimie 84:413–421.

609 58. Pommier S, Gavioli M, Cascales E, Lloubes R. 2005. Tol-dependent macromolecule
610 import through the *Escherichia coli* cell envelope requires the presence of an exposed TolA
611 binding motif. J Bacteriol 187:7526–7534.

612 59. Karlsson F, Borrebaeck CAK, Nilsson N, Malmberg-Hager A-C. 2003. The
613 Mechanism of bacterial infection by filamentous phages involves molecular interactions
614 between TolA and phage protein 3 domains. J Bacteriol 185:2628–2634.

615 60. Germon P, Clavel T, Vianney A, Portalier R, Lazzaroni JC. 1998. Mutational analysis
616 of the *Escherichia coli* K-12 TolA N-terminal region and characterization of its TolQ-
617 interacting domain by genetic suppression. J Bacteriol 180:6433–6439.

618 61. Koebnik R. 1993. The molecular interaction between components of the TonB-
619 ExbBD-dependent and of the TolQRA-dependent bacterial uptake systems. Mol Microbiol

- 620 9:219.
- 621 62. Goemaere EL, Cascales E, Lloubès R. 2007. Mutational Analyses Define Helix
622 Organization and key residues of a bacterial membrane energy-transducing complex. J Mol
623 Biol 366:1424–1436.
- 624 63. Klebba PE. 2016. ROSET Model of TonB action in Gram-Negative bacterial iron
625 acquisition. J Bacteriol 198:1013–1021.
- 626 64. Possot OM, Letellier L, Pugsley AP. 1997. Energy requirement for pullulanase
627 secretion by the main terminal branch of the general secretory pathway. Mol Microbiol
628 24:457–464.
- 629 65. Yamamoto M, Kanegasaki S, Yoshikawa M. 1981. Role of membrane potential and
630 ATP in complex formation between *Escherichia coli* male cells and filamentous phage fd.
631 Microbiology 123:343–349.
- 632 66. Labedan B, Goldberg EB. 1979. Requirement for membrane potential in injection of
633 phage T4 DNA. Proc Natl Acad Sci USA 76:4669–4673.
- 634 67. Maki-Yonekura S, Matsuoka R, Yamashita Y, Shimizu H, Tanaka M, Iwabuki F,
635 Yonekura K. 2018. Hexameric and pentameric complexes of the ExbBD energizer in the Ton
636 system. eLife 7:e35419.
- 637 68. Miller, Jeffrey H. 1992. A short course in bacterial genetics: a laboratory manual and
638 handbook for *Escherichia coli* and related bacteria. Cold Spring Harbor Laboratory Press,
639 Plainview, NY.

640

641

642 **LEGEND TO FIGURES**

643

Figure 1. Schematic representation of the two homologous proton-motive force coupled systems. **a.** The different components of the Tol-Pal and the Ton-ExbB-ExbD are presented according to previously published literature. **b.** Periplasmic view of TolA, TolR and TolQ TM segment organization. While the system has been described to show a stoichiometry of 1 TolA, 2 TolR and 4-6 TolQ, here only one protein of each is shown for clarity. The interfacial area delimitating the hypothetical aqueous channel is light grey. Residues predicted to be important for proton conductivity are indicated on TolQ TM2, TolQ TM3 and TolR TM segments. Residues S18 and H22 described as involved in energy transduction from the TolQ-TolR motor to TolA are part of an SHLS motif and indicated on TolA TM domain. TBDT: TonB-dependent transporter.

Figure 2. Phenotypic analysis of *E. coli* GM1 wild-type strain and *tol* mutants used in this study. **A.** Cells sensitivity to SDS is reported as the percentage of growth for each strain cultivated with 0.2% SDS, compared to the same strain grown in LB medium. Experiments were conducted in triplicate. **B.** Colicin sensitivity was estimated by 10-fold serial spot dilutions. One microlitre of colicin (A, E1 or B) was spotted on to a growing lawn of cells. Clear zones indicate cell death. ColA and ColE1 are dependent on the Tol system while ColB is dependent on the TonB-ExbBD system for uptake.

Figure 3. Sensitivity to Fd-Tc phage and infection frequency for the WT, $\Delta tolA$, $\Delta tolQR$ (**A**) and $\Delta tolQR\Delta exbBD$ strains (**B**). Cells were incubated with the phage during 30 min, and 10-fold serial diluted and spotted on LB plates (left pannel) and on LB plates supplemented with tetracyclin (LB+Tc, right pannel), in order to numerate the total number of CFU, and Fd phage infected CFU, respectively. Experiments were conducted in triplicate. The frequency of infection (F) indicated on the right was calculated as the mean of the 3 infection with standard deviation.

669

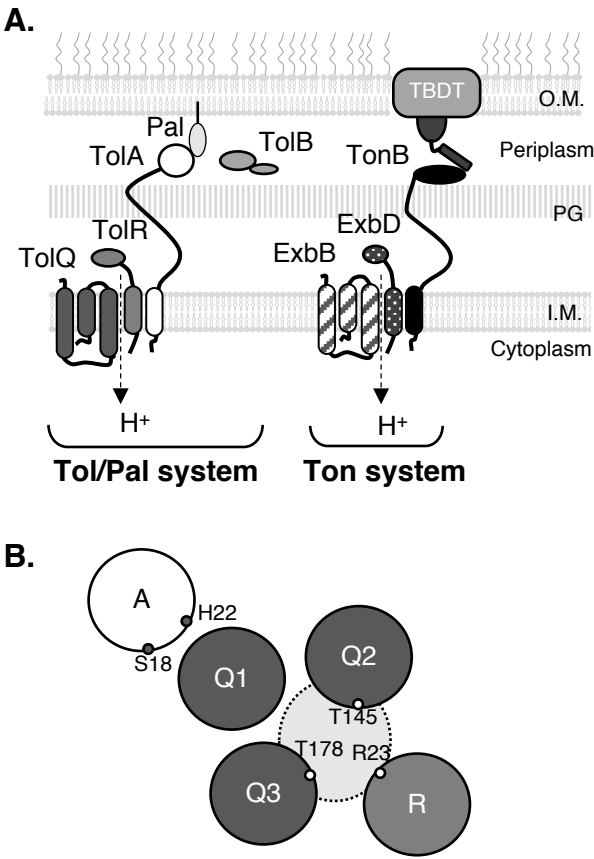
670 Figure 4. Phenotypic characterization of various strains producing the isolated TolA receptor
671 domain for the phage (TolAIII) in the periplasm, compared to a control protein PIII^{ΔYGT} unable
672 to bind TolA. **A.** Cells sensitivity to SDS is reported as the percentage of growth for each strain
673 cultivated with 0.2% SDS, compared to the same strain grown in LB medium. Experiments
674 were conducted in triplicate. **B.** Sensitivity to Fd-Tc phage and infection frequency were
675 determined as indicated in Figure 3.

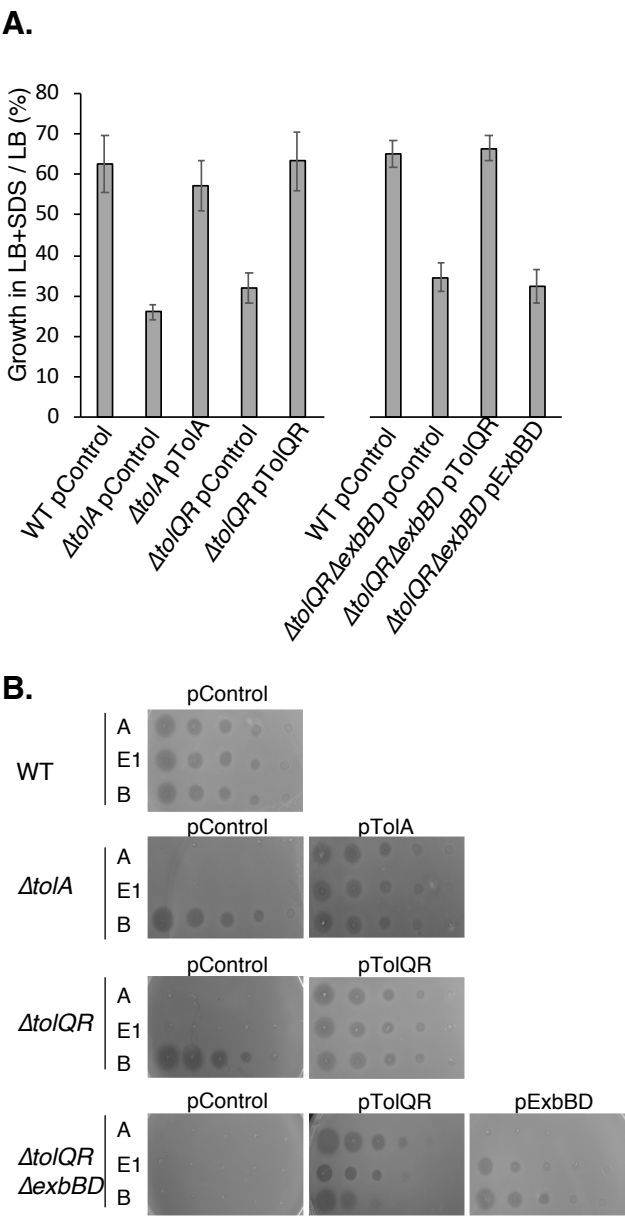
676

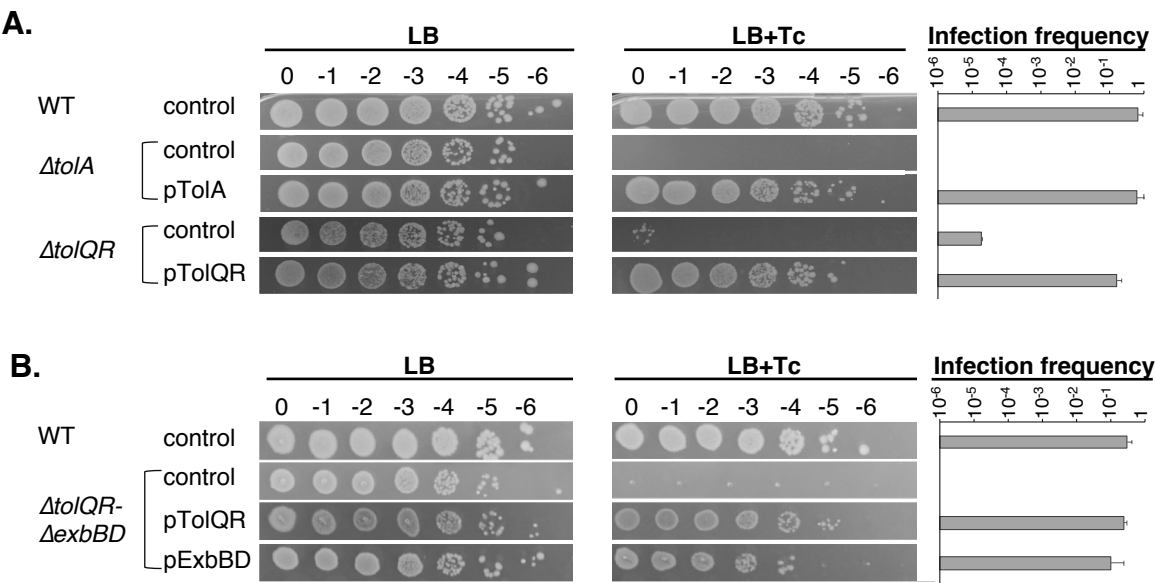
677 Figure 5. Phenotypic consequences of the production of TolQ, TolR and TolA, or their variants
678 in the $\Delta tolQR\Delta tolA\Delta exbBD$ mutant background. **A.** Sensitivity to colicins and percentage of
679 growth in the presence of 0.2% SDS compared to standard LB conditions. **B.** Colicin sensitivity
680 was estimated by 10-fold serial spot dilutions, as indicated in Figure 2. **C.** Sensitivity to Fd-Tc
681 phage and infection frequency. Experiments were conducted as indicated in Figure 3.

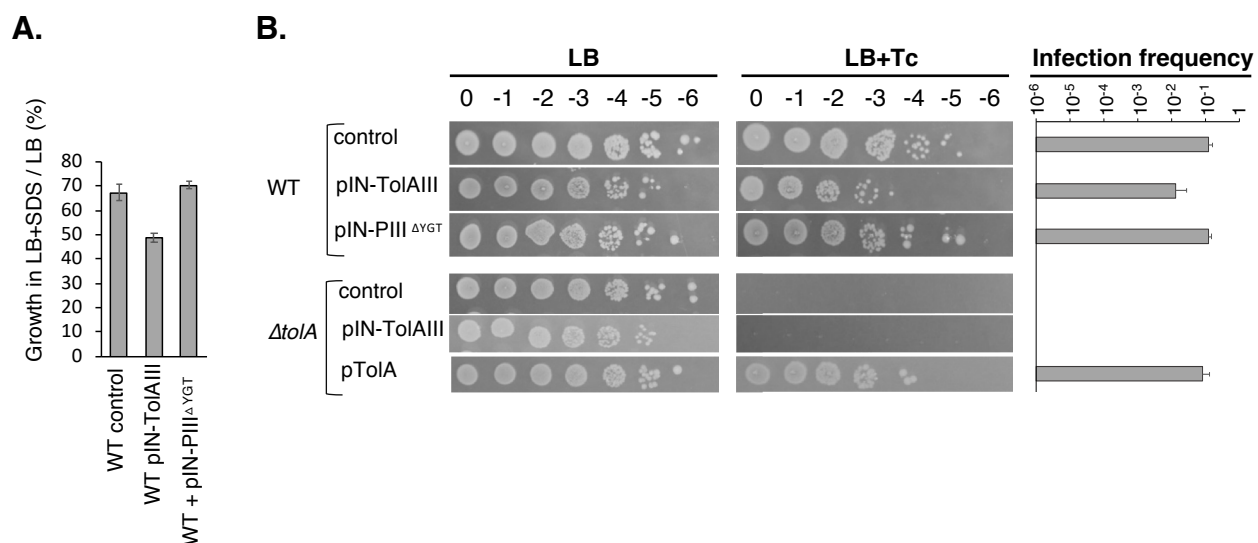
682

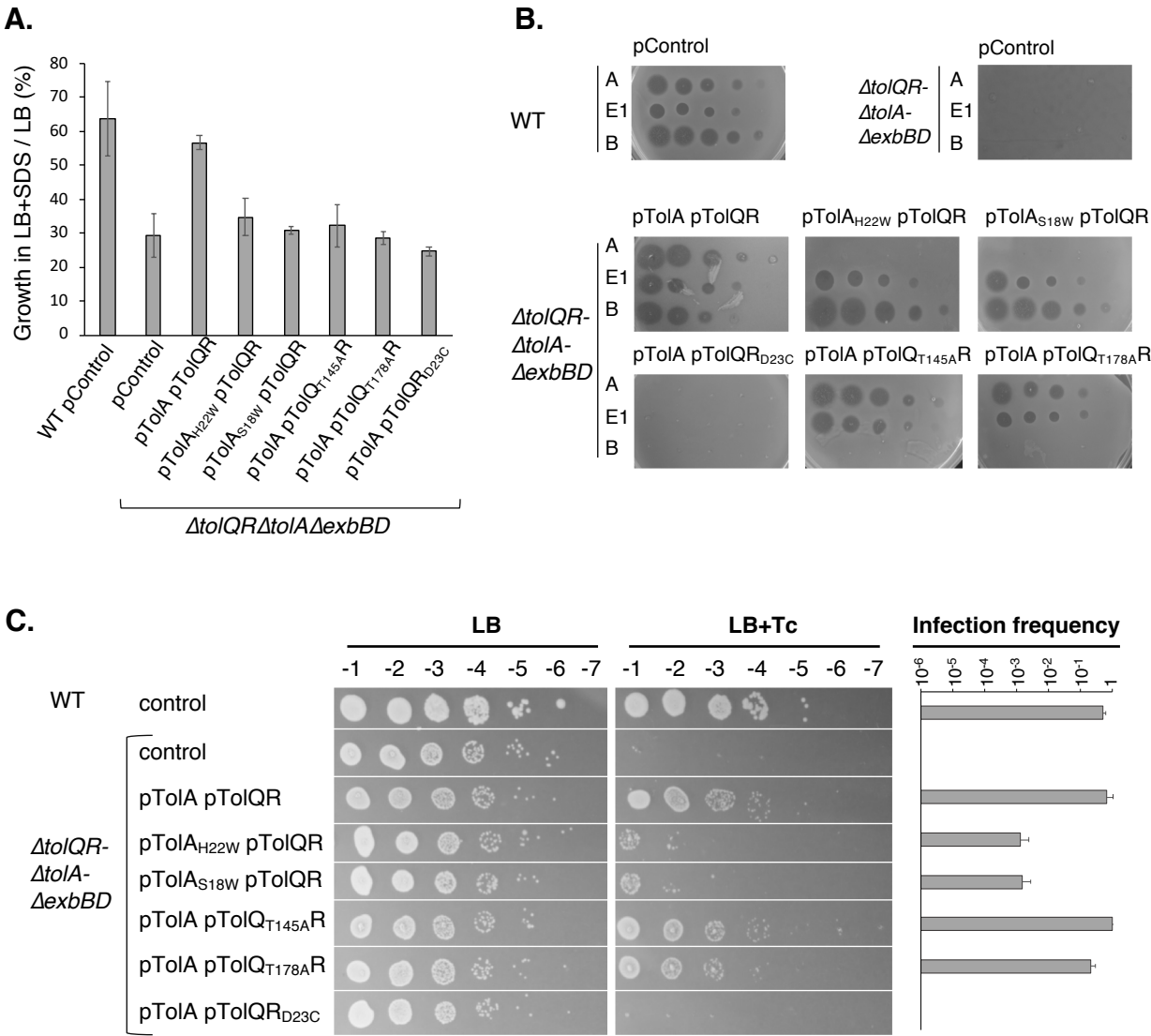
683











Supplemental data

Decoupling filamentous phage uptake and energy of the TolQRA motor in *Escherichia coli*.

Poutoum SAMIRE, Bastien SERRANO, Denis DUCHE, Emeline LEMARIE, Roland LLOUBES,
Laetitia HOUOT

Table S1 : Strains and plasmids used in the study.

Table S2 : Primers used in the study

Supplemental Figure 1

Supplemental Figure 2

Supplemental Figure 3

Supplemental Figure 4

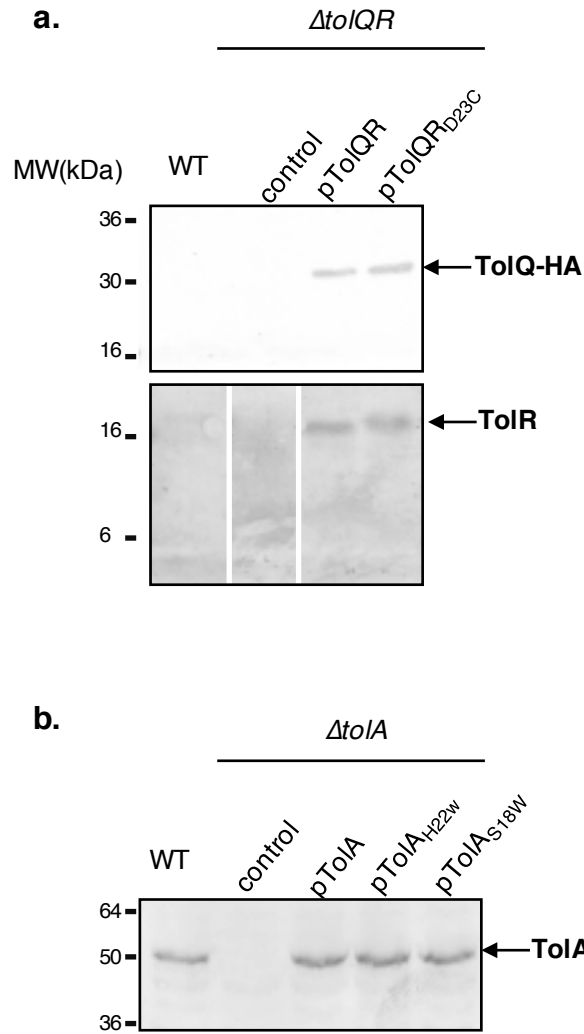
References

Table S1 : Strains and plasmids used in the study.

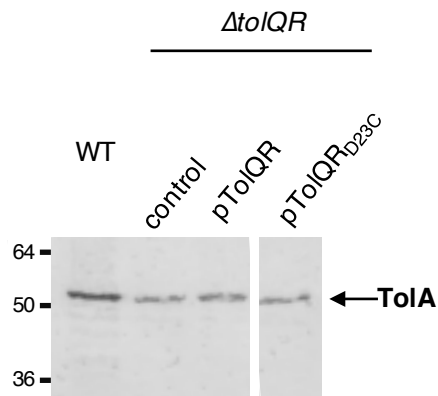
<i>E. coli</i> strains and phage	Genotype or description	Source/References
DH5α	F- Φ80/ <i>lacZ</i> ΔM15 Δ(<i>lacZYA-argF</i>) U169 <i>recA1 endA1 hsdR17</i> (rK ⁻ , mK ⁺) <i>phoA supE44 λ- thi-1 gyrA96 relA1</i>	Laboratory collection
W3110 Δ <i>tolA</i>	W3110 strain deleted of <i>tolA</i> gene	(1)
W3110 Δ <i>tolQR</i>	W3110 strain deleted of <i>tolQ</i> and <i>tolR</i> genes.	(1)
W3110 Δ <i>exbBD</i>	W3110 strain deleted of <i>exbB</i> and <i>exbD</i> genes	(1)
GM1	<i>ara, thi, Δ(lac pro), F', lac, pro</i>	Laboratory collection
GM1 Δ <i>tolA</i>	GM1 strain deleted of <i>tolA</i> gene	This study
GM1 Δ <i>tolQR</i>	GM1 strain deleted of <i>tolQ</i> and <i>tolR</i> genes.	This study
GM1 Δ <i>tolQRA</i>	GM1 strain deleted of <i>tolQ</i> , <i>tolR</i> and <i>tolA</i> genes.	This study
GM1 Δ <i>tolQRΔexbBD</i>	GM1 strain deleted of <i>tolQ</i> , <i>tolR</i> and <i>exbB</i> , <i>exbD</i> genes	This study
GM1 Δ <i>tolQRAΔexbBD</i>	GM1 strain deleted of <i>tolQ</i> , <i>tolR</i> , <i>tolA</i> and <i>exbB</i> , <i>exbD</i> genes	This study
Fd-tet	Fd phage carrying a tetracyclin resistance gene	ATCC 37000
<u>Plasmids used in rescue experiments</u>		
pOK12	IPTG-inducible plasmid, KanR	Vieira and Messing, 1991
pTolA	pOK12 carrying the <i>tolA</i> gene from <i>E. coli</i> , KmR	This study, A. Barnéoud-Arnoulet
pTolA _{S18W}	ptolA bearing a S-to-W substitution at position 18, KmR	This study
pTolA _{H22W}	ptolA bearing a H-to-W substitution at position 22, KmR	This study
pBAD/HisC	pBR322-derived expression vector, L-arabinose inducible, AmpR	Invitrogen
pTolQR	pBAD/HisC carrying the <i>E. coli tolQ</i> gene fused to an HA tag and the <i>tolR</i> gene, AmpR	(1)
pTolQR _{T145AR}	pTolQR bearing a T-to-A substitution at position 145 in TolQ, AmpR	This study
pTolQR _{T178AR}	pTolQR bearing a T-to-A substitution at position 178 in TolQ, AmpR	This study
pTolQR _{D23C}	pTolQR bearing a D-to-C substitution at position 23 in TolR, AmpR	(1)
pExbBD	pKE61 plasmid, pT7-5 derivative carrying the <i>E. coli exbB</i> and <i>exbD</i> genes, AmpR	K.Eick-Helmerich
<u>Plasmids used for periplasmic expression</u>		
pIN	pIN-III-ompA2 vector, <i>ompA</i> signal sequence followed by a multi cloning site, ApR	Laboratory collection
pIN-PIII ^{ΔYGT}	pIN vector carrying fragment of phage PIII encoding gene and deleted of the YGT motif, N-terminal Strep Tag epitope, C-terminal 6-His epitope, ApR	(2)
pIN-TolAIII	pIN vector carrying a fragment of <i>tolA</i> sequence coding for the Fd phage receptor domain, ApR	(3)

Table S2 : Primers used in the study

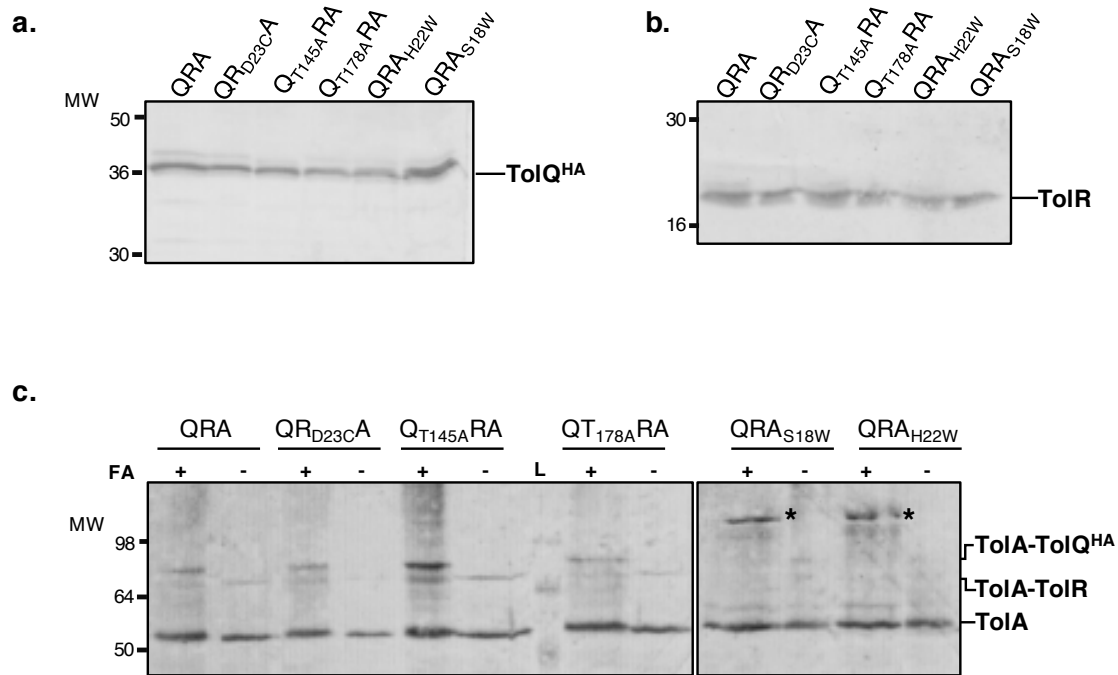
PRIMERS	SEQUENCES
Quick Change mutagenesis	
TolA (S18W)	CGGGCGATAATTATTTGGGCAGTGCTGCATGTC GACATGCAGCACTGCCCAAATAATTATCGCCCG
TolA (H22W)	ATTCAGCAGTGCTGTGGGTCATCTTATTTGCG CGCAAATAAGATGACCCACAGCACTGCTGAAAT
TolQ (T145A)	ACAGACCAATATACGGGCTGATGGAGCCAACCGTACCGAGGAAC TCAGCCCGTATATTGGTCTGTTTGGCGCGGTCTGGGGGATCATGCACG
TolQ (T178A)	TCAACGCTTCTGCGATACCGGGCGCAACCATTTGCAGTGTTGCTT CCCGGTATCGCAGAAGCGTTGATTGCAGCTGCAATTGGTCTGTTTGCCG



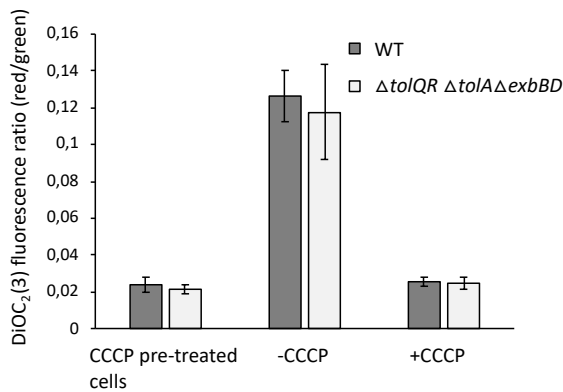
Supplemental Figure 1. Protein production level of HA-tagged TolQ, of TolR (panel a) and of TolA protein (panel b) in various strain backgrounds. Western immunoblot of 0.2 OD units of whole-cell lysates of *E. coli* GM1 F⁺ wild-type strain, $\Delta tolQR$ and $\Delta tolA$ mutant strains carrying various inducible expression vectors, and probed with monoclonal anti-HA, or polyclonal anti-TolR or anti-TolA antibodies. The empty control plasmids are pBAD-His/C (panel a) and pOK12 (panel b). The molecular weight markers (in kDa) are indicated on the left.



Supplemental Figure 2. Protein production level of TolA in *E. coli* GM1 F⁺ wild-type strain and in $\Delta tolQR$ mutant strain background carrying various l-arabinose inducible expression vectors. 0.2 OD units were loaded on a 12.5% acrylamide SDS-PAGE and immunodetected using anti-TolA polyclonal antibody. The empty pBAD-His/C plasmid is used as control. Molecular mass markers (in kDa) are indicated on the left.



Supplemental Figure 3. Protein production and TolQRA complex formation in a GM1 F⁺ $\Delta tolQRA \Delta exbBD$ mutant strain expressing either the wild-type copy of TolQ^{HA}, TolR and TolA, or point mutant variants. 0.2 uOD were loaded on a 12.5% acrylamide SDS-PAGE and immunodetected using anti HA antibody (**a**), anti-TolR polyclonal antibody (**b**) or anti-TolA polyclonal antibody (**c**). In pannel **c**, *in vivo* formaldehyde (FA) cross-linking of cells is indicated as (+). The composition of complexes detected, as previously determined (4, 5), is indicated on the right. Molecular mass markers (in kDa) are indicated on the left. Asterisk (*) denotes a complex of high molecular mass that has been previously proposed to be a dimer of TolA. L: Protein ladder.



Supplemental Figure 4. Membrane potential measurements. The membrane potential across the inner-membrane of the WT and the $\Delta tolQR \Delta tolA \Delta exbBD$ strains was investigated by using the fluorescent probe diethyloxacarbocyanine iodide (DiOC2(3), ThermoFisher #D14730). DiOC2(3) exhibits green fluorescence when incorporated into bacterial cells, but the fluorescence shifts toward red emission as the dye molecules self-associate at the higher cytosolic concentrations caused by larger membrane potentials. The proton ionophores CCCP destroys membrane potential by eliminating the proton gradient, allowing calibration of the experiment. While the relative amount of red and green fluorescence signal will vary with cell size and aggregation, the ratio of red/green fluorescence signal can be used as a size-independent measurement of membrane potential. Briefly, LB broth was inoculated with an overnight culture of the required *E. coli* strain and incubated with shaking at 37 °C until the OD600 reached 0.5. The cells were harvested by centrifugation (8000 g for 3 min) at room temperature and concentrated to an OD600 ~1.0 in PBS. 1 mL culture was loaded with 1mM EDTA just before adding 20 μ M DiOC2(3) in DMSO, and incubated for 20 min at room temperature in the dark. Cultures were then centrifuged for 3 min at 8,000g and subsequently washed twice with 1 mL PBS to remove extracellular dye, before the cells were resuspended in 1 mL PBS. A spectrofluorimeter was used to measure green fluorescence (488 nm/530 nm) and shifts to red fluorescence (488 nm/610 nm). The red/green signal ration was recorded (graph bars -CCCP). Then, the membrane potential was disrupted by the addition of CCCP (5 μ M) during 10 min and the signal was recorded (graph bars +CCCP).

As a positive control for membrane depolarization, cultures were treated with 5 μ M of CCCP during 10 min before adding the dye (graph bars CCCP pre-treated cells). A sample treated with DMSO only was used to determine background signal. Each condition was measured in triplicate.

References

- 1- Petiti M, Serrano B, Faure L, Lloubes R, Mignot T, Duché D. 2019. Tol energy-driven localization of Pal and anchoring to the peptidoglycan promote outer-membrane constriction. *J Mol Biol* 431:3275-3288.
- 2- Pommier S, Gavioli M, Cascales E, Lloubes R. 2005. Tol-dependent macromolecule import through the *Escherichia coli* cell envelope requires the presence of an exposed TolA binding motif. *J Bacteriol* 187:7526–7534.
- 3- Bouveret E, Journet L, Walburger A, Cascales E, Bénédicti H, Lloubès R. 2002. Analysis of the *Escherichia coli* Tol-Pal and TonB systems by periplasmic production of Tol, TonB, colicin, or phage capsid soluble domains. *Biochimie* 84:413–421.
- 4- Derouiche R, Bénédicti H, Lazzaroni JC, Lazdunski C, Lloubès R. 1995. Protein complex within *Escherichia coli* inner membrane. TolA N-terminal domain interacts with TolQ and TolR proteins. *J Biol Chem* 270:11078–11084.
- 5- Germon P, Clavel T, Vianney A, Portalier R, Lazzaroni JC. 1998. Mutational analysis of the *Escherichia coli* K-12 TolA N-terminal region and characterization of its TolQ-interacting domain by genetic suppression. *J Bacteriol* 180:6433–6439.